Emergence of Topological Fermi Liquid from a Strongly Correlated Bosonic System in Optical Superlattices

Bo-lun Chen and Su-peng Kou*
Department of Physics, Beijing Normal University, Beijing 100875, China

Recent experiments on quantum degenerate gases give an opportunity for simulating strongly-correlated electronic systems in optical lattices. It may shed light on some long-standing puzzles in condensed-matter physics, like the nature of high-temperature superconductivity in cuprates that had baffled people over two decades. It is believed that the two-dimensional fermionic Hubbard model, or t-J model, contains the key to this problem; but the difficulty of unveiling the mystery of a strongly-interacting fermionic system is also generally acknowledged. Here, as a substitute, we systematically analyze the property of bosonic t-J model simulated in optical superlattices near unit-filling. In particular, we show the emergence of a strange topological Fermi liquid with Fermi surfaces from a purely bosonic system. We also discuss the possibility of observing these phenomena in ultracold atom experiments. The result may provide some crucial insights into the origin of high-T_c superconductivity.

PACS numbers: 03.75.Hh, 03.75.Lm, 64.60.Cn, 74.20.-z, 74.20.Mn

In recent years, the physics community has witnessed a series of exciting discoveries and achievements. Among them, using ultracold atoms that form Bose-Einstein Condensates (BEC) or Fermi degenerate gases to make precise measurements and simulations of quantum many-body systems, is quite impressive and has become a rapidly-developing field[1, 2]. Since atoms are cooled down to temperature near absolute zero and trapped in optical lattices building from six orthogonal laser beams, they provide us a peaceful playground for manipulating atoms with unprecedented accuracy. Some pioneering works[3] revealed the promising potential of applying ultracold atoms to make quantum computer and quantum simulator: By changing the intensity, phase and polarization of incident laser beams, one can tune the Hamiltonian parameters including the dimension, the hopping strength and the particle interaction at will. People have successfully observed the Mott insulator–superfluid transition in both bosonic[4] and fermionic[5, 6] degenerate gases, and have demonstrated how to produce[7] and control effective spin interactions in a double-well ensemble[8]. All these evidences imply that an era in which atomic and optical physics unites with condensed-matter physics is within sight.

Particularly, the two-dimensional fermionic Hubbard model (or t-J model) is one of the most interesting issues depicting the nature of high-temperature superconductivity[9, 10, 11]. Ever since the discovery of high T_c cuprates, tremendous efforts had been contributed to investigations of this model. Derived from Hubbard model at half-filling (one electron per site), the t-J model describes the motion of doped holes in an antiferromagnetic (AF) background. It carries the essence of a strongly correlated electronic system with intrinsic competition between superexchange interaction of spins and hopping processes of charge-carriers (holes). Over the past two decades, people have employed many methods and developed different schemes, hoping to fully understand this model. Although a lot of consensus have been accomplished, there are still some ambiguities to be clarified. For example, can superconductivity evolve from a purely fermionic repulsive many-body system? Are there exist some new phases of matter in high-T_c superconductors?

Therefore, some people suggest to use its bosonic counterpart, the bosonic t-J model[12, 13, 14], as a trial model to investigate, for bosons are much more easier to deal with in both analytic and numerical approaches. After obtaining some experiences and conclusions, we may use them as reminders and analogies to original fermionic model. Besides, considering the present situation of experiments in ultracold atoms, where bosons are more accessible to be cooled and controlled, we believe it is worthwhile to explore the bosonic t-J model in optical lattices which can be formally written into two parts:

$$\hat{H} = \hat{H}_t + \hat{H}_J = -t \sum_{\langle ij\rangle\sigma} (\hat{a}^\dagger_{i\sigma}\hat{a}_{j\sigma} + H.c.) + J \sum_{\langle ij\rangle} \hat{\mathbf{S}}_i \cdot \hat{\mathbf{S}}_j, \quad (1)$$

where Hilbert space is restricted by the no-double-occupancy constraint $\sum_\sigma \hat{a}^\dagger_{i\sigma}\hat{a}_{i\sigma} \leq 1$, $\hat{a}_{i\sigma}$ annihilates a two-component boson ($\sigma \equiv \uparrow, \downarrow$ denoting two internal states) and $\hat{\mathbf{S}}_i$ is the (pseudo)spin operator at site i, $\hat{\mathbf{S}}_i = \frac{1}{2}\sum_{\alpha\beta} \hat{a}^\dagger_{i\alpha}\sigma_{\alpha\beta}\hat{a}_{i\beta}$ with Pauli matrix $\sigma = (\sigma^x, \sigma^y, \sigma^z)$, $\langle ij\rangle$ denotes the nearest-neighboring counting. $\hat{H}_t$ and $\hat{H}_J$ describes hopping ($t > 0$) and an effective AF superexchange ($J > 0$) interactions respectively.

In a seminal experiment[8], Bloch *et al.* loaded a two-component ^{87}Rb condensate, $|F = 1, m_F = 1\rangle$ ($\uparrow$) and $|F = 1, m_F = -1\rangle$ ($\downarrow$), into arrays of isolated double wells. By changing the relative phase of the two laser standing waves, the potential difference Δ in one double-well can be raised or ramped down. The oscillation of the condensate after such manipulation contained infor-

*Corresponding author; Electronic address: spkou@bnu.edu.cn

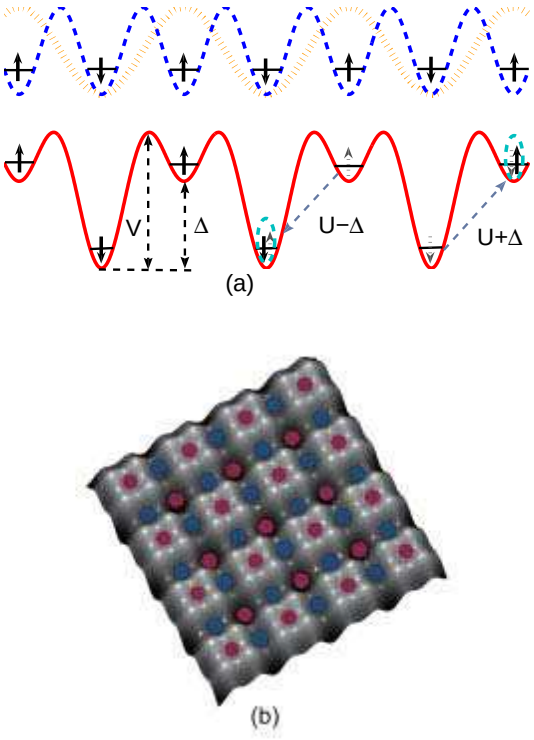

FIG. 1: Illustrations of optical superlattices. (a) Construction of an optical superlattice. Combining two sets of optical lattices (wavelength λ and 2λ) with a relative phase difference π to produce a superlattice. V is the depth of the potential well. The superexchange processes are realized through virtual hoppings, resulting perturbations $U \pm \Delta$ in the Hamiltonian. (b) A visualization of a 2D superlattice, blue atoms denote one spin species ($|\uparrow\rangle$) and red atoms denote the other species ($|\downarrow\rangle$).

mation of the strength and sign of the effective superexchange energy J. With proper bias Δ, they could convert ferromagnetic interaction ($J < 0$) into antiferromagnetic one ($J > 0$).

To implement a controllable hopping term, we have to generalize the double-wells to a set of biased optical superlattices. As illustrated in Fig. (1), for instance, we can start from the situation with one boson per site, different species in neighboring sites. Then by adding another set of optical lattice adiabatically, whose wavelength is as twice as the original one and has a relative phase difference of π, we can build a superlattice (with shallow sites and deep sites), where a certain type of bosons being trapped in a certain type of sites, for instance, $|\uparrow\rangle$ in shallow sites and $|\downarrow\rangle$ in its neighboring deep sites.

By changing the shape of the superlattice, one can lift the potential difference Δ to a fixed value to realize the effective AF superexchange interaction ($J > 0$). Furthermore, by adjusting the relative phase and polarization between incident lasers, one can control the tunneling amplitude $t_{i\sigma}$ of different inner states of atoms in different sites to be identical. Therefore, we can introduce the hopping effect while keeping a(n) (inhomogeneous) Heisenberg-type interaction in an optical superlattice. (see Methods for details.)

In addition, according to ref. [15], one can introduce vacancies in a BEC trapped in one-dimensional (1D) optical lattice by pointing an electron beam at specific sites to remove atoms. Due to the small diameter ($100 \sim 150$ nm) of the electron beam compared with the lattice spacing, holes can be doped in without additional losses in other sites. The final occupying configuration can be visualized with highly spatial resolution through scanning electron microscopy. Since single-occupancy has been achieved in current experiments[8, 16] as an initial setup, we believe that this technique can be further extended to 2D and 3D superlattices loaded with multi-component atoms, thus one can manipulate and(or) remove different species deliberately and observe the dynamics of holes with single-atom, single-site sensitivity. Above all, the realization of theoretical model (1) as well as the necessary doping technique are all within reach in current experiments.

The main analysis is arranged as follows: for bosonic t-J Hamiltonian near unit-filling, we analyze the doping effect in a topological perspective. We show the existence of several exotic phases as vacancies being gradually introduced. Then we discuss how to detect these features in currently-available techniques in ultracold atom experiments.

I. HOLONS: BOSONS OR FERMIONS?

At unit-filling, the bosonic t-J model is simple and can be reduced to AF Heisenberg model, $\hat{H} = J \sum_{\langle ij \rangle} \hat{\mathbf{S}}_i \cdot \hat{\mathbf{S}}_j$. A variational wave-function based on Resonating Valence Bond (RVB) picture by using Schwinger-boson description can produce[17, 18, 19] an unrivaled accurate ground-state energy; a generalized version[18] can further provide the staggered magnetization and spin excitation spectrum precisely. So the bosonic RVB picture is a natural choice for describing AF Heisenberg model. Explicitly, we can introduced two flavors of bosons on each site, created by a canonical operator $\hat{b}^\dagger_{i\sigma}$ acting on the vacuum $|0\rangle$ without bosons, satisfying $\hat{b}^\dagger_{i\sigma}\hat{b}_{i\sigma} = 1$. This representation is equivalent to the following operator identity between the spin and boson operators $\hat{\mathbf{S}}_i = \frac{1}{2}\hat{\mathbf{b}}^\dagger_i \sigma \hat{\mathbf{b}}_i$. Here $\hat{\mathbf{b}}_i = (\hat{b}_{i\uparrow}, \hat{b}_{i\downarrow})^T$ is a bosonic spinon annihilation operator. The mean-field value is characterized by a bosonic RVB order parameter $\Delta^s_{ij} = \langle \hat{b}_{i\sigma}\hat{b}_{j,-\sigma}\rangle \neq 0$ for the nearest-neighbor sites, which depicts the short-range AF correlation as $\langle \hat{\mathbf{S}}_i \cdot \hat{\mathbf{S}}_j \rangle = -\frac{1}{2}|\Delta^s_{ij}|^2$. At zero temperature, spinon $\hat{\mathbf{b}}$ becomes massless and Bose-condensation takes place with $\langle \hat{\mathbf{b}} \rangle \neq 0$, corresponding to the long-range Néel order in x-y plane.

To learn the property of an AF order with vacancies, we should generalize the idea of *spin-charge sep-*

aration, which has become a very basic concept in understanding the doped Mott insulator related to high-T_c cuprate[10, 20]. Unlike a usual quasi-particle that carries both spin and charge quantum numbers in conventional metals, it states that the system has two independent elementary excitations, the neutral spinon and the spinless holon. It is assumed that usual quasi-particle excitations may no longer be stable against the spin-charge separation mechanism once being created, e.g., by injecting a bare vacancy into the system; and it has to decay into more elementary spinons and holons. In other words, to theoretically describe the introduction of a single vacancy, one has to first annihilate a particle state $|\Psi\rangle$ together with a bosonic spinon $\hat{b}_{i\sigma}$, then generate a spinless operator $\hat{h}_i^\dagger$ denotes a holon (a vacancy) as

$$\hat{a}_{i\sigma}\,|\Psi\rangle = \hat{h}_i^\dagger \hat{b}_{i\sigma}\,|\Psi\rangle\,,\ |\Psi\rangle = \prod_{i\sigma}\hat{b}_{i\sigma}^\dagger|0\rangle. \tag{2}$$

In addition, $\hat{h}_i^\dagger$ and $\hat{b}_{i\sigma}$ should satisfy the no-double-occupancy constraint, $\hat{h}_i^\dagger\hat{h}_i + \sum_\sigma \hat{b}_{i\sigma}^\dagger\hat{b}_{i\sigma} = 1$. In contract to the case of high-T_c cuprates, holons in bosonic t-J model are neutral for they are actually the absence of cold atoms in a certain site.

However, the situation changes when the hole moves. According to Marshall[21], the ground-state wave function of the Heisenberg Hamiltonian for a bipartite lattice satisfies a sign rule. It requires that flips of two antiparallel spins at nearest-neighbor sites are always accompanied by a sign change in the wave function: $|\cdots\uparrow\downarrow\cdots\rangle \mapsto (-1)\times|\cdots\downarrow\uparrow\cdots\rangle$. To show the sign effect in detail, we divide a bipartite lattice into odd (A) and even (B) sublattices and assign an extra sign (-1) to every down spin at A site. When the hole initially locating at site i hops onto a nearest-neighbor site j, the Marshall sign rule is violated, resulting in a string of mismatched signs on the vacancy's course[22]. The spin wave function is changed into

$$|\Psi\rangle \mapsto |\tilde{\Psi}\rangle = (-1)^{\sum_i \hat{n}^b_{i\in A,\downarrow}}\,|\Psi\rangle\,,$$

where $\hat{n}^b_{i\in A,\downarrow} = \hat{b}^\dagger_{i\in A,\downarrow}\hat{b}_{i\in A,\downarrow}$ is the number of down spin on each A-sublattice. In particular, if the hole moves through a closed path C on the lattice to return to its original position, it will get a Berry phase $(-1)^{N_C^\downarrow}$, where $N_C^\downarrow$ is the total number of down spins "encountered" by the hole on the closed path C.[23, 24, 25] This process is illustrated in Fig. (2a).

To deal with this unavoidable Berry phase $(-1)^{N_C^\downarrow}$ in the ground-state wave function when there is mobile hole, we introduce a phase-string transformation[23] $|\tilde{\Psi}\rangle \mapsto e^{i\hat{\Theta}}|\tilde{\Psi}\rangle = |\Psi\rangle$, where $\hat{\Theta} = \sum_{ij}\theta_{ij}\hat{n}_i^h\hat{n}_{j\downarrow}^b$, $\hat{n}_i^h$ and $\hat{n}_{j\downarrow}^b$ are occupation number operators of the hole and down-spins, with a phase factor θ_{ij} =Im[ln$(z_i - z_j)$]. Here $z \equiv x + iy$ denotes position and the subscripts i and j denote lattice sites. Considering the single-occupancy constraint, $\hat{\Theta} = -\frac{1}{2}\sum_{ij}\hat{n}_i^h\theta_{ij}[1 - \hat{n}_j^h - \sum_\sigma(-1)^\sigma\,\hat{n}_{j\sigma}^b]$, where $(-1)^\uparrow \equiv 1$, $(-1)^\downarrow \equiv -1$. The phase-shift factor $e^{i\hat{\Theta}}$ can also be regarded as a unitary transformation on an arbitrary operator: $\hat{O} \mapsto e^{i\hat{\Theta}}\hat{O}e^{-i\hat{\Theta}}$. For example, operators of holons $\hat{h}_i^\dagger$ and spinons $\hat{b}_{i\sigma}$ are transformed as follow,

$$\begin{aligned} e^{i\hat{\Theta}}\hat{h}_i^\dagger e^{-i\hat{\Theta}} &= \hat{h}_i^\dagger e^{-i\sum_j\theta_{ij}\hat{n}_j^h + \frac{i}{2}\sum_{j\sigma}(-1)^\sigma\theta_{ij}\hat{n}_{j\sigma}^b - \frac{i}{2}\sum_j\theta_{ij}}, \\ e^{i\hat{\Theta}}\hat{b}_{i\sigma}e^{-i\hat{\Theta}} &= \hat{b}_{i\sigma}e^{-\frac{i}{2}\sum_j(-1)^\sigma\theta_{ij}\hat{n}_j^h}. \end{aligned}$$

Now we have restored the simple spin wave function $|\Psi\rangle$ as equation (2) originally defined, but have got a set of nontrivial operators, and it is just the aim of the above transformation.

Furthermore, by defining $\hat{h}_i'^\dagger = \hat{h}_i^\dagger e^{-i\sum_j\theta_{ij}\hat{n}_j^h}$, we can see that except for a phase factor $e^{\frac{i}{2}\sum_j\theta_{ij}}$, holon $\hat{h}_i$ and spinon $\hat{b}_{i\sigma}$ are symmetric,

$$\begin{aligned} \hat{h}_i &\mapsto \hat{h}_i' e^{-\frac{i}{2}\sum_{j\sigma}(-1)^\sigma\theta_{ij}\hat{n}_{j\sigma}^b} \times e^{\frac{i}{2}\sum_j\theta_{ij}}, \\ \hat{b}_{i\sigma} &\mapsto \hat{b}_{i\sigma}e^{-\frac{i}{2}\sum_j(-1)^\sigma\theta_{ij}\hat{n}_j^h}; \end{aligned} \tag{3}$$

namely, $\hat{h}_i \overset{h\to b,\ i\to i\sigma}{\longmapsto} \hat{b}_{i\sigma}$ and $\hat{b}_{i\sigma} \overset{b\to h,\ i\sigma\to i}{\longmapsto} \hat{h}_i$. The phase factor $e^{\frac{i}{2}\sum_j\theta_{ij}}$ means an additional lattice π-flux-per-plaquette for holons. From equation (3), one can see that there exists a mutual semionic statistics between holons and spinons, where holons perceive spinons as π-vortices and vice versa. In particular, after the transformation $\hat{h}_i'^\dagger = \hat{h}_i^\dagger e^{-i\sum_j\theta_{ij}\hat{n}_j^h}$, $\hat{h}_i'^\dagger$ obeys fermionic anti-commutation[26],

$$\{\hat{h}_i'^\dagger, \hat{h}_j'\} = \delta_{ij}.$$

Finally, based on the RVB ground state by considering the phase string effect[23, 24, 25], the effective Hamiltonian of holons in bosonic t-J model can be written as

$$\begin{aligned} \hat{H}_h &= -t_h\sum_{\langle ij\rangle}(e^{i\hat{a}_{ij} - i\phi_{ij}^0}\hat{h}_i'^\dagger\hat{h}_j' + H.c.) + \\ &\quad \frac{\Delta}{2}\sum_i(-1)^i\,\hat{h}_i'^\dagger\hat{h}_i' + \mu\sum_i\hat{h}_i'^\dagger\hat{h}_i', \end{aligned} \tag{4}$$

where $t_h \approx |\Delta_{ij}^s|t$ is the effective hopping amplitude of holons, μ is the chemical potential. The gauge field $\hat{a}_{ij}$ satisfy the topological constraint $\sum_C\hat{a}_{ij} = \pm\pi\sum_{l\in C}(\hat{n}_{l\uparrow}^b - \hat{n}_{l\downarrow}^b)$ for a closed loop C, ϕ_{ij}^0 describes a π flux per plaquette, $\sum_\square\phi_{ij}^0 = \pm\pi$. It is obvious that the difference between fermionic t-J model and bosonic t-J model is the statistic of holons: in former case, holons are bosons; and in latter case, they are fermions.

Now we may be able to answer the question: what is the fate of a holon in an AF order? As we have mentioned above, the AF order lying in x-y plane can be seen as a Bose condensation of spinons, $\langle\hat{b}_{i\sigma}\rangle \neq 0$. According to the above effective Hamiltonian (4), and the quantity $\hat{S}_i^\dagger = (-1)^i\hat{b}_{i\uparrow}^\dagger\hat{b}_{i\downarrow}e^{i\sum_j\theta_{ij}\hat{n}_j^h}$, a holon introduced here is a topological defect carrying spin twists and changing its peripheral spin configuration, as a meron-like object[27,

28, 29, 30], such a spin vortex (for a holon at the origin) may be characterized by a unit vector $\mathbf{n}_i = (-1)^i \langle \mathbf{S}_i \rangle / S$,

$$\mathbf{n}_i = \frac{\mathbf{r}_i}{|\mathbf{r}_i|}, \ \mathbf{r}_i^2 = x_i^2 + y_i^2.$$

This meron-like spin configuration is schematically shown in Fig. (2b).

By now, one may imagine that a single hole would become a meron in a long-range AF order. However, the answer is not quite right. For a single meron configuration, the energy is logarithmically divergent, $E \approx J|\Delta_{ij}^s| \ln(L/a_0)$ with L the size of the system. In order to remove this infinite-energy cost, as in the present case, each holon-meron has to "nucleate" an anti-meron from the background spontaneously. Define $n_i^x + i n_i^y = e^{i\phi_0 + i\phi_i}$, with the unit vector $\mathbf{n}_0 \equiv (\cos\phi_0, \sin\phi_0)$ as the magnetization direction at infinity. In presence of a fermionic holon centered at $-z_k/2$ and an anti-meron centered at $z_k/2$, we have[31, 32] $\phi_i^k = \mathrm{Im} \ln[(z_i - z_k/2)/(z_i + z_k/2)]$ with $z_k \equiv e_k^x + i e_k^y$. By using $\hat{\mathbf{e}}_k = (e_k^x, e_k^y)$ to denote the spatial displacement of the holon and anti-meron centered, a *dipolar* spin configuration at a sufficiently large distance is obtained,

$$\phi_i \approx \frac{(\hat{\mathbf{z}} \times \hat{\mathbf{e}}_k) \cdot \mathbf{r}_i}{|\mathbf{r}_i|^2}, \ |\mathbf{r}_i| \gg |\hat{\mathbf{e}}_k|.$$

Thus, each pair of holons and anti-merons forms a composite, as shown in Fig. (2c). In contrast to the logarithmically divergent meron-energy, the energy a dipole E_d becomes finite[31, 32], $E_d \approx J|\Delta_{ij}^s| \ln[(|\hat{\mathbf{e}}_k| + a_0)/a_0]$, $|\hat{\mathbf{e}}_k| \gtrsim a_0$.

Physically, one may consider a bare hole (spinless holon) created by an annihilation operator $\hat{h}^\dagger$ at point a, then it may jump to point b via some discrete steps, being connected by a phase string in between. Since the holon can reach b through different virtual paths originated at a, this singular phase string is then replaced by, or relaxes to, a smooth *dipole* configuration. An anti-meron itself is a semi-vortex formed by condensed spinons and it is immobile. Therefore, the hole-dipole as a whole must remain localized (self-trapped) in space. The resulting spin configuration has a dipolar symmetry while the distortion of the direction of magnetization is long ranged and decays as r^{-1}[32, 33].

II. TOPOLOGICAL FERMI LIQUID

In the lightly doped region, $\delta \to 0$, there exist localized holes that are self-trapped around anti-merons via a logarithmically confining potential $V(r) \approx q^2 \ln(|\mathbf{r}|/a)$, $q^2 = 2\pi J|\Delta_{ij}^s|$, and their dipolar moments are randomly distributed. Such kind of AF ordered state with random dipoles has been studied in refs. [31, 36, 37, 38]. It is known that when $T = 0$, the spin-correlation length is finite for arbitrary doping δ. This implies the destruction of long-range AF order, as long as $\delta > 0$. Consequently,

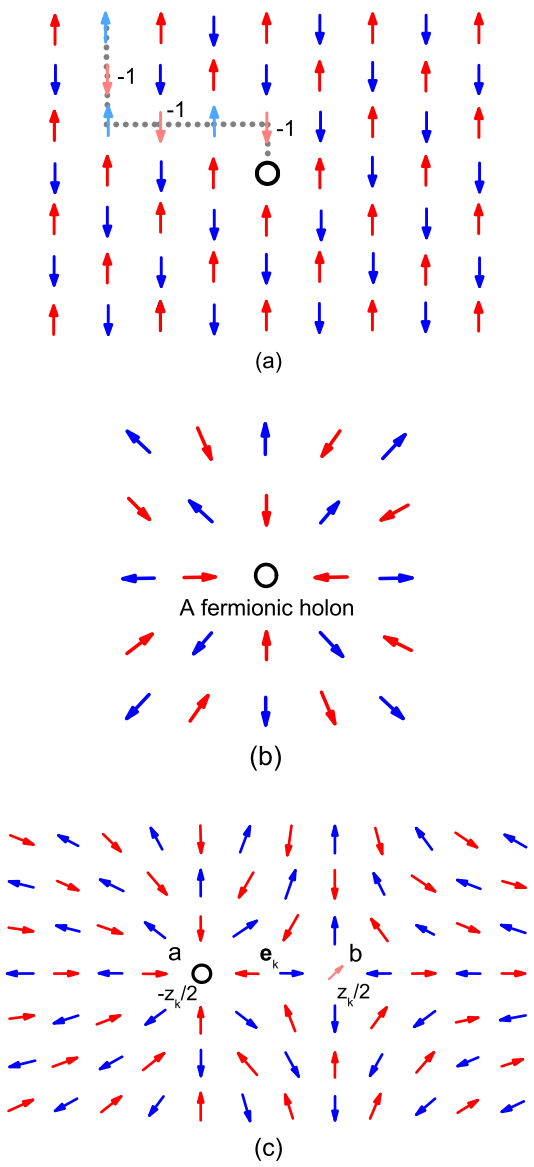

FIG. 2: (a) A schematic demonstration of the phase string effect on a long-range AF order background. The point in $A\,(B)$-sublattice is denoted by red(blue) arrows. The double-dot path is the course that a hole (black open circle) moves through. For clarity, spins on this path is plotted in light colors. Once the hole's hopping results a down spin on A-sublattice, there is a sign change (-1) over the wave function $|\Psi\rangle$, as described in the text. (b) An illustration of a meron configuration. Due to the mutual statistics, the vacancy has become a fermionic particle. (c) An illustration of a holon-dipole configuration. It is a confined object composed of a holon-meron and an anti-meron at two poles: $a\,(-z_k/2)$ and $b\,(z_k/2)$, connected by a branch-cut with the spatial separation $\hat{\mathbf{e}}_k$ as a dipole moment.

AF order is limited mainly in finite sizes, where the size ξ of a domain is determined by the hole's concentration, $\xi \approx a/\sqrt{\delta}$. Accordingly, this state has been termed as a cluster spin glass[39, 40]. The spin glass freezing temperature is then expected to vary as $T_g \propto \xi^2 \propto a^2/\delta$, below which holons tend to form a glass and their dynamics strongly slows down.

When doping increases, more and more dipoles appear. As a result, the "confining" potential $V(r)$ between these dipoles will be screened by polarizations of pairs lying between them. When this screening effect becomes so strong that even the largest pair has to break up, holons and anti-merons are liberated to move individually. This qualitative analysis suggests that a localization-delocalization phase transition should occur at a critical point δ_c, in a fashion of the Kosterlitz-Thouless (KT) transition. Using the renormalization group method[31, 35], one can determine the critical hole density $\delta_c = \delta_c(T)$ or temperature $T_{\rm de} = T_{\rm de}(\delta)$ at which dipoles collapse and holon-merons are "deconfined" from the bound state with anti-merons. At zero temperature, the critical hole density has been numerically determined as

$$\delta_c(T=0) \approx \frac{0.84}{2\pi^2} = 0.043.$$

Therefore, a zero-temperature quantum critical point exists at $\delta_c = 0.043$ where hole-dipoles dissolve into holon-merons and anti-merons.

When $\delta > 0.043$, fermionic holons are delocalized, so a Fermi surface emerges in the momentum space. And since two holons always *repulse* each other, for they are merons with *same* topological charges, then these fermions cannot pair with each other and it makes the Fermi surface stable. This is different from the case where electrons form Cooper pairs in superconductors, because here we have topological repulsions not electronic repulsions.

Thus, we display the global phase-diagram of bosonic t-J model in Fig. (3). There exists three different regions globally: region I, AF insulator, $\delta = 0$; region II, insulating spin-glass (SG), $\delta \in (0, 0.043)$; region III, topological Fermi-liquid (TFL) phase with spin-liquid ground state, $\delta \in (0.043, 0.5)$. The phase boundary that protects the physics in low doping regimes can be written as $k_B T \approx c\,(1-2\delta)\,J$, c is an integration quantity (see Methods). Particularly, our results illustrate the emergence of an exotic fermionic state (TFL) in a pure bosonic system.

In TFL state, the effective Hamiltonian of holons can be written as

$$\hat{H}_h = -t_h \sum_{\langle ij \rangle} e^{i\phi^0_{ij}} \hat{h}'^{\dagger}_i \hat{h}'_j + \frac{\Delta}{2} \sum_i (-1)^i \hat{h}'^{\dagger}_i \hat{h}'_i + \mu \sum_i \hat{h}'^{\dagger}_i \hat{h}'_i,$$

and the dispersion relation is

$$E_k = \mu \pm \frac{1}{2}\sqrt{16 t_h^2 \left[\cos^2(k_x) + \cos^2(k_y)\right] + \Delta^2},$$

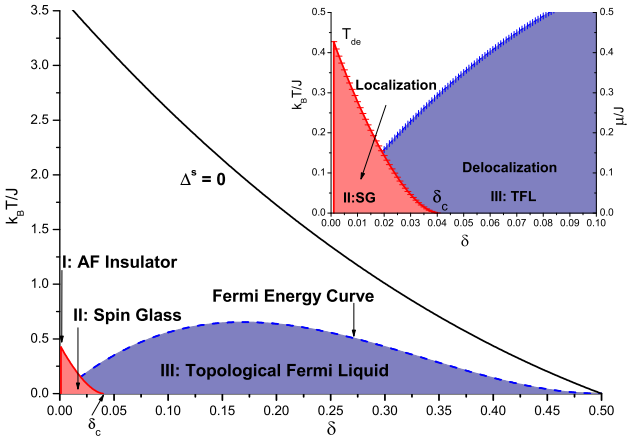

FIG. 3: The global phase diagram. The solid black line indicates the phase boundary where $|\Delta^s_{ij}| = 0$. Different regions are demonstrated in the text. The inset depicts detailed phase boundaries as well as the quantum critical point δ_c in low doping region ($\delta < 0.1$). The Fermi energy curve $\mu(\delta)$ implies the existence of Fermi surface of deconfined holons. It is scaled by the superexchange energy J as shown in the inset, where we have chosen $U/t = 12$, namely, $t/J = 3$ and $\Delta/J = 50$.

as Fig. (4) shows.

In Fig. (5), we show the evolution of Fermi surfaces by plotting four doping cases, $\delta = 0.05$, 0.1, 0.15 and 0.2, respectively. From the global phase diagram Fig. (3) and Fig. (5), we suggest that in experiments people may observe TFL in bosonic t-J model of 15% hole concentration, of which highest Fermi energy with clear Fermi surfaces are predicted.

Besides, when holon moves, the spin configuration changes simultaneously, thus there is no long-range AF order anymore. Instead, the magnetic ground-state becomes a spin liquid state with invariant spin-rotation and translation symmetry. Without anti-merons matching with holons, holons exert an "effective magnetic field" on spinons (recall the mutual relation between the two excitations), $B_h = \pi\rho_h$ with ρ_h the density of holons. Hence, a new length scale is introduced to the spinon system, which is the magnetic cyclotron length $l_c = B_h^{-1/2}$. l_c will later be connected to the remaining magnetic correlation length.

As we mentioned above, doping creates a Landau-level structure in the spinon spectrum. Thus, low-lying spin fluctuations are expected to be sensitive to dopants. After calculations, we find

$$\chi''(\mathbf{q},\omega) \sim \chi''(\mathbf{Q}_0,\omega)\, e^{-|\mathbf{q}-\mathbf{Q}_0|^2 l_c^2/2}.$$

Here $\chi''(\mathbf{q},\omega)$ is defined as ($\beta = 1/k_B T$)

$$\chi''(\mathbf{q},\omega) = \frac{1}{2}\left(1 - e^{-\omega\beta}\right) \int dt d\mathbf{r} e^{i(\omega t - \mathbf{q}\cdot\mathbf{r})} \langle \mathbf{S}(\mathbf{r},t) \cdot \mathbf{S}(0,0) \rangle \quad (5)$$

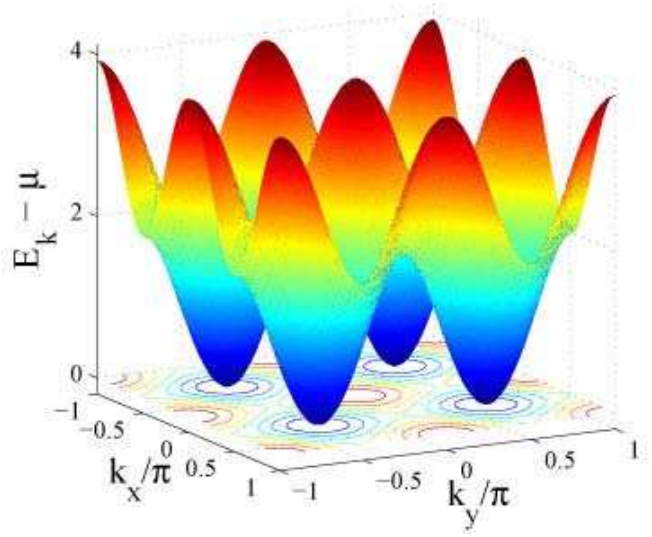

FIG. 4: The dispersion relation of the topological Fermi liquid. The relative energy $E_k - \mu$ of the upper branch is shown in the unit of t with $\Delta/t = 20$.

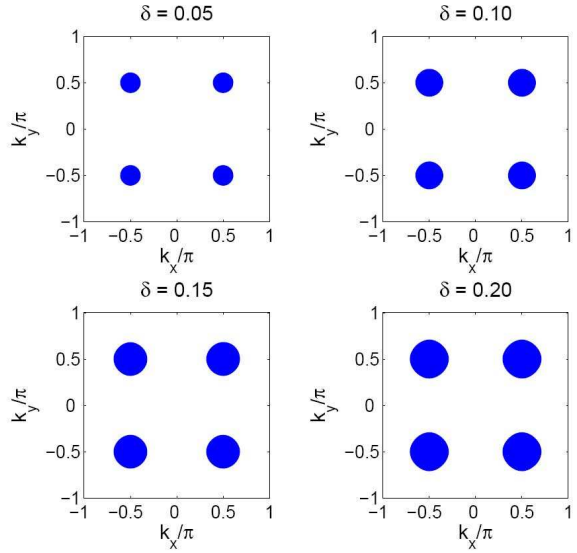

FIG. 5: Illustrations of Fermi surfaces. The doping concentrations are shown as titles of individual plots.

where $\langle \mathbf{S}(\mathbf{r},t)\cdot\mathbf{S}(0,0)\rangle$ is the spin-spin correlation function. This is a Gaussian type around the AF wavevector $\mathbf{Q}_0 = (\pm\pi,\pm\pi)/a_0$ with a width l_c^{-1}. Consequently, it determines the spin-spin correlation in the real space as $\cos(\mathbf{Q}_0\cdot\mathbf{r})\, e^{-|\mathbf{r}|^2/\xi^2}$, where the correlation length $\xi = \sqrt{2}l_c = a_0\sqrt{2/(\pi\delta)}$ is in the same order of the average hole-hole distance[41]. Namely, doped holes break up the long-range AF correlation into short-range AF fragments within a length scale of ξ.

In contrast, the ground-state of fermionic t-J model is a superconducting state of condensed holons, in which spin liquid state is always masked by holons' condensation[42]. While in bosonic t-J model, it is the topological Fermi liquid state with massless fermionic excitations, in which one can easily detect properties of this spin liquid state. For these reasons, the observation of this exotic quantum state (TFL with short range spin correlation) in bosonic t-J model may pave an alternative approach to verify the microscopic theory of high T_c superconductivity.

III. DETECTIONS AND SUMMARY

In region I and II, the system is an insulator in the first place, so the momentum distribution is universal and isotropic in the Brillouin zone (without considering the trapping and boundary conditions). This feature can be detected by measuring density profile measurement[44], or via Bragg spectroscopy[43] to observe the momentum spectrum. Additionally, in the Néel state (I), the condensate exhibits long range AF order, while in the spin glass state (II), this long ranged magnetic order disappears. This difference can be distinguished through spatial spin-spin correlations, $\langle \hat{S}_z(\mathbf{r}_1)\hat{S}_z(\mathbf{r}_2)\rangle$. As demonstrated in refs.[45, 46], using a probe laser beam which goes through the condensate, one can measure the phase shift or change of polarization of the outgoing beam $\langle \hat{X}_{\text{out}}\rangle$ to obtain the magnetization $\langle \hat{X}_{\text{out}}\rangle \propto \langle \hat{M}_z\rangle \propto \int d\mathbf{r}\phi(\mathbf{r})\langle \hat{S}_z(\mathbf{r})\rangle$, where $\phi(\mathbf{r})$ is the spatial intensity profile of the laser beam. The quantum noise $\langle \hat{X}^2_{\text{out}}\rangle \propto \langle \hat{M}_z^2\rangle \propto \int d\mathbf{r}_1 d\mathbf{r}_2 \phi(\mathbf{r}_1)\phi(\mathbf{r}_2)\langle \hat{S}_z(\mathbf{r}_1)\rangle\langle \hat{S}_z(\mathbf{r}_2)\rangle$ reveals the atomic correlations in the system. This method can directly examine the existence of 2D AF correlations.

In region III, we have demonstrated that one natural characteristic of TFL is the existence of Fermi surfaces in the Brillouin zone. Esslinger et al.[47] had successfully observed the Fermi surface in a 3D optical lattice filled with fermionic atoms. Similarly, one may also observe these Fermi levels in our bosonic system, as shown in Fig. (5). Besides, the short-range AF fluctuations may also be observed. As equation (5) indicates, the spin dynamic structure factor as well as the dynamic spin susceptibility function are linked with spin-spin correlations. The latter one reflects the effective short-range magnetic correlation length ξ.

To sum up, in this paper, we first demonstrate the implementation of bosonic t-J model in optical superlattices filled with a two-component BEC. And for the first time, we systematically discussed the possible quantum phases of this model upon doping. A key feature is the mutual semionic statistics between the two elementary excitations of the system, holons and spinons. When there are only a few holes around, they tend to form hole-dipoles, locally changing the underlying spin texture into meron-anti-meron pairs. At low doping, the

deformed spin configuration loses the long-range order, and there emerges a spin glass state. When holes are prevailing, through a quantum phase transition ($\delta_c = 0.043$) that frees those self-localized holons in spin glass state, a strange topological Fermi liquid with Fermi surface appears in a purely bosonic system, as a significant result of the mutual statistics between holons and spinons. We also list accessible experimental approaches to verify and detect these novel theoretical predictions.

IV. METHODS

A. Perturbation Theory in Large U Limit

The two-component Bose-Hubbard model in a biased superlattice can be generally written as

$$\begin{aligned}\hat{H} &= -t\sum_{\langle ij\rangle\sigma}[\hat{a}^{\dagger}_{i\sigma}\hat{a}_{j\sigma} + H.c. + \frac{\Delta}{2t_\sigma}(\hat{n}_{i\sigma} - \hat{n}_{j\sigma})] + \\ & U\sum_i \hat{n}_{i\uparrow}\hat{n}_{i\downarrow} + \frac{U'}{2}\sum_i \hat{n}_{i\sigma}(\hat{n}_{i\sigma} - 1), \end{aligned} \quad (6)$$

where $t = \sqrt{16/\pi}E_r\left(V/E_r\right)^{3/4}e^{-2\sqrt{V/E_r}}$[7] with atomic recoil energy $E_r = \hbar^2k^2/2m$, k is the wave vector of laser, m is the atomic mass, V describes external potential. The inter-species repulsion is defined as $U = \sqrt{8/\pi}ka_sE_r\left(V/E_r\right)^{3/4}$ with a_s the s-wave scattering length among species, and the intra-species repulsion is $U' = \sqrt{8/\pi}ka'_sE_r\left(V/E_r\right)^{3/4}$, a'_s is the corresponding scattering length. This term vanishes at exact unit-filling, but can contribute in higher-order tunneling processes.

In the large U limit ($U \gg t$) and nearly unit-filling $n \lesssim 1$, which is actually a prerequisite for building the aforementioned superlattices and is naturally satisfied, the hopping term can be treated as a perturbation. Thus, we introduce two projection operator: $\mathcal{P}$ projects the initial Hilbert space onto the single-occupancy subspace $(|0\rangle_i, |\uparrow\rangle_i, |\downarrow\rangle_i)$, $\mathcal{Q} = 1 - \mathcal{P}$ projects onto the double-occupancy subspace $(|\uparrow\downarrow\rangle_i)$. We further divide equation (6) into $\hat{H}_0 + \hat{T}_{\rm mix}$, where $\hat{H}_0$ describes processes in $\mathcal{P}$ subspace and $\hat{T}_{\rm mix}$ mixes the upper and lower band via virtual tunnelings.

Applying canonical transformation $\hat{H}_{\rm eff} = e^{-\hat{S}}\hat{H}e^{\hat{S}}$ and eliminating first order terms of $\hat{T}_{\rm mix}$, we find

$$\begin{aligned}\hat{H}_{\rm eff} &= \hat{H}_0 + \frac{1}{2}\left[\hat{T}_{\rm mix}, \hat{S}\right], \\ \hat{S} &= \sum_{mn}|m\rangle\langle m|\left(\frac{\hat{T}_{\rm mix}}{E_n - E_m}\right)|n\rangle\langle n|.\end{aligned}$$

The projector $|\epsilon\rangle\langle\epsilon|$ can be chosen as $\mathcal{P}$ and $\mathcal{Q}$. Energy differences between upper and lower band are $E_{\mathcal{Q}} - E_{\mathcal{P}} \approx U \pm \Delta, \frac{U'}{2} \pm \Delta$ thus $\hat{S} = (\tilde{U}^{-1} + 2\tilde{U'}^{-1})(\mathcal{P}\hat{T}\mathcal{Q} - \mathcal{Q}\hat{T}\mathcal{P})$ with $\tilde{U} = U - \Delta^2/U$, $\tilde{U}' = U' - \Delta^2/U'$. After calculating the detailed terms, we can obtain the effective Hamiltonian as

$$\begin{aligned}\hat{H}_{\rm eff} &= -t\sum_{\langle ij\rangle\sigma}(\hat{a}^{\dagger}_{i\sigma}\hat{a}_{j\sigma} + H.c.) + \\ & \sum_{\langle ij\rangle}[J_z\hat{S}^z_i\hat{S}^z_j - J_\perp(\hat{S}^x_i\hat{S}^x_j + \hat{S}^y_i\hat{S}^y_j)], \end{aligned} \quad (7)$$

where

$$J_z = \frac{4t^2}{\tilde{U}} - \frac{8t^2}{\tilde{U}'}, J_\perp = \frac{4t^2}{\tilde{U}}.$$

When a_s and a'_s do not differ very much (this condition can somehow be realized in experiments),

$$J_z \approx -\frac{4t^2}{\tilde{U}} + \epsilon$$

with ϵ denoting a small spatial inhomogeneity. In fact, this small inhomogeneity is necessary in our following discussions, for it can be seen as an analogy for the effective inter-layer-coupling in high-T_c cuprates.

At the first glance, it seems that bosons (say, $|\uparrow\rangle$) in shallow sites may hop to neighboring deep sites more easily due to lower energy barrier they feel, comparing their counterparts ($|\downarrow\rangle$) in the reverse process. However, thanks to spin-dependent controlling techniques, which can be achieved by adjusting parameters of incident light beams, one can regulate tunneling amplitudes of different species, making atoms in different sites feel a similar hopping matrix element, $t_\uparrow = t_\downarrow \equiv t$. This is the reason we straightforwardly set an identical hopping term t at the beginning.

Meanwhile, to achieve an effective AF superexchange interaction, we need to set $\Delta = \sqrt{2}U$ ($\tilde{U} = -U$) to change signs of coefficients: $J_z \approx 4t^2/U + \epsilon$, $J_\perp = -4t^2/U$ in equation (7). As a result, the global coefficient of spin interaction becomes positive, $J \approx 4t^2/U$, as equation (1) asks.

Under these circumstances, we finally derive the bosonic t-J model with a small inhomogeneity in z direction, which can be formally written as equation (1). Quite recently, two papers [49, 50] suggested a similar proposal and made detailed discussions.

B. Mean field calculation from slave-particle approach

This representation is equivalent to the following operator identity between the spin and boson operators. Defining $\hat{a}_{i\sigma} = \hat{h}^{\dagger}_i e^{i\hat{\Theta}^{\rm string}_{i\sigma}}\hat{b}_{i\sigma}$ and $\hat{\mathbf{S}}_i = \frac{1}{2}\hat{\mathbf{b}}^{\dagger}_i\sigma\hat{\mathbf{b}}_i$, where $\hat{h}^{\dagger}_i$ creates a fermionic holon, leaving a non-local phase string and $\hat{b}_{i\sigma}$ annihilates a bosonic (Schwinger-boson) spinon

at site i, we rewrite equation (1) as $\hat{H} = \hat{H}_h + \hat{H}_s$:

$$\begin{aligned}\hat{H}_h &= -t\sum_{\langle ij\rangle\sigma} e^{i\hat{A}^f_{ij}}\hat{h}^\dagger_i\hat{h}_j e^{i\hat{A}^f_{ji}}\hat{b}^\dagger_{j\sigma}\hat{b}_{i\sigma},\\ \hat{H}_s &= -\frac{J}{2}\sum_{\langle ij\rangle\sigma\sigma'} e^{i\hat{A}^h_{ij}}\hat{b}^\dagger_{i\sigma}\hat{b}^\dagger_{j,-\sigma}e^{i\hat{A}^h_{ji}}\hat{b}_{j,-\sigma'}\hat{b}_{i\sigma'},\end{aligned}$$

Here $\hat{\Theta}^{\rm string}_{i\sigma} = \frac{1}{2}(\hat{\Phi}^b_i - \sigma\hat{\Phi}^h_i)$ is a topological phase with the contribution from spinon number $\hat{n}^b_\sigma$, $\hat{\Phi}^b_i = \sum_{l\neq i,\sigma}(-1)^\sigma \,\mathrm{Im}\left[\ln\left(z_i - z_l\right)\right]\hat{n}^b_{l\sigma}$ and the holon's ($\hat{n}^h$) contribution, $\hat{\Phi}^h_i = \sum_{l\neq i}\mathrm{Im}\left[\ln\left(z_i - z_l\right)\right]\hat{n}^h$. And $\hat{A}^f_{ij}$ and $\hat{A}^h_{ij}$ describe quantized fluxes bounded to spinons and holons. We then introduce a mean-field bosonic RVB order parameter $\Delta^s = \sum_\sigma\langle e^{-i\sigma\hat{A}^h_{ij}}\hat{b}_{i\sigma}\hat{b}_{j,-\sigma}\rangle$, and take the constraint on total spinon number and dilute effect into account, we apply mean-field approximation on $\hat{H}$ and solve two self-consistent equations:

$$\begin{aligned}\delta &= 2 - \frac{1}{N}\sum_k \lambda_k E_k^{-1}\coth\left(\beta E_k/2\right),\\ \Delta^s &= \frac{1-2\delta}{N}\sum_k \xi_k^2 J_s^{-1}E_k^{-1}\coth\left(\beta E_k/2\right),\end{aligned}$$

to obtain the phase boundary

$$k_BT = 2J\left(1-2\delta\right)\left(2-\delta\right)\left(\ln\frac{3-\delta}{1-\delta}\right)^{-1}$$

that separates $\Delta^s = 0$ and $\Delta^s \neq 0$. Here N is the total lattice number. Detailed definitions can be found in ref. [24].

Acknowledgments

The authors thank Z.-Y. Weng, Y.-B. Zhang, B. Wu, W.-M. Liu for helpful discussions and comments. This research is supported by NCET and NFSC Grant no. 10574014, 10874017.

[1] Bloch, I., Dalibard, J. & Zwerger, W. Many-body physics with ultracold gases. *Rev. Mod. Phys.* **80,** 885 (2008).

[2] Giorgini, S., Pitaevskii, L. P. & Stringari, S. Theory of ultracold atomic Fermi gases. *Rev. Mod. Phys.* **80,** 1215 (2008).

[3] Jaksch, D. & Zoller, P. The cold atom Hubbard toolbox. *Annals of Physics* **315 (1),** 52-79 (2005) and references therein.

[4] Greiner, M., Mandel, O., Esslinger, T., Hänsch, T. W. & Bloch, I. Quantum phase transition from a superfluid to a Mott insulator in a gas of ultracold atoms. *Nature* **415,** 39-44 (2002).

[5] Jödens, R., Strohmaier, N., Günter, K., Moritz, H. & Esslinger, T. A Mott insulator of fermionic atoms in an optical lattice. *Nature* **455,** 204-207 (2008).

[6] Schneider, U. et al. Metallic and Insulating Phases of Repulsively Interacting Fermions in a 3D Optical Lattice. arXiv: 0809.1464.

[7] Duan, L.-M., Demler, E. & Lukin, M. D. Controlling spin exchange interactions of ultracold atoms in optical lattices. *Phys. Rev. Lett.* **91,** 090402 (2003).

[8] Trotzky, S. et al. Time-resolved observation and control of superexchange interactions with ultracold atoms in optical lattices. *Science* **319,** 295-299 (2008).

[9] Hirsch, J. E. Attractive interaction and pairing in fermion systems with strong on-site repulsion. *Phys. Rev. Lett.* **54,** 1317-1320 (1985).

[10] Anderson, P. W. The resonating valence bond state in La_2CuO_4 and superconductivity. *Science*, **235,** 1196-1198 (1987).

[11] Zhang, F. C. & Rice, T. M. Effective Hamiltonian for the superconducting Cu oxides. *Phys. Rev. B* **37,** 3759-3761 (1988).

[12] Boninsegni, M. Phase separation and stripes in a boson version of a doped quantum antiferromagnet. *Phys. Rev. B* **65,** 134403 (2002).

[13] Boninsegni, M. & Prokof'ev, N. V. Phase diagram of an anisotropic bosonic t-J model. *Phys. Rev. B* **77,** 092502 (2008).

[14] Aoki, K., Sakakibara, K., Ichinose, I. & Matsui, T. Magnetic order and superconductivity in the bosonic t-J model of CP^1 spinons and doped bosonic holons. arXiv: 0811.2845.

[15] Gericket, T., Würtz, P., Reitz, D., Langen, T. & Ott, H. High-resolution scanning electron microscopy of an ultracold quantum gas. *Nat. Phys.* doi:10.1038/nphys1102 (2008).

[16] Volz, T. et al. Preparation of a quantum state with one molecule at each site of an optical lattice. *Nat. Phys.* **2,** 692-694 (2006).

[17] Liang, S., Doucot B. & Anderson, P. W. Some new variational resonating-valence-bond-type wave functions for the spin-$\frac{1}{2}$ antiferromagnetic Heisenberg model on a square lattice. *Phys. Rev. Lett.* **61,** 365-368 (1988).

[18] Chen, Y.-C. & Xiu, K. Optimized RVB states of the 2-d antiferromagnet: ground state and excitation spectrum. *Phys. Lett. A* **181,** 373-380 (1993).

[19] Auerbach, A. *Interacting Electrons and Quantum Magnetism* Ch. 5 (Springer Verlag, New York, 1994).

[20] Kivelson, S. A., Rokhsar, D. S. & Sethna, J. R. Topology of the resonating valence-bond state: solitons and high-T_c superconductivity. *Phys. Rev. B* **35,** 8865-8868 (1987).

[21] Marshall, W. Antiferromagnetism. *Proc. Roy. Soc. (London) A* **232**, 48-68 (1955).

[22] Trugman, S. Interaction of holes in a Hubbard antiferro-

magnet and high-temperature superconductivity. *Phys. Rev. B* **37,** 1597-1603 (1988).

[23] Sheng, D.-N., Chen, Y.-C. & Weng, Z.-Y. Phase string effect in a doped antiferromagnet. *Phys. Rev. Lett.* **77,** 5102-5105 (1996).

[24] Weng, Z.-Y., Sheng D.-N. & Ting, C.-S. Bosonic resonating-valence-bond description of a doped antiferromagnet. *Phys. Rev. Lett.* **80,** 5401-5404 (1998).

[25] Weng, Z.-Y., Sheng, D.-N, Chen, Y.-C & Ting, C.-S. Phase string effect in the t-J model: general theory. *Phys. Rev. B* **55,** 3894-3906 (1997).

[26] The emergent fermionic excitations has been pointed out in another full bosonic system in Ref. [48]. However, the mechanism in Ref. [48] is much different from ours, both the Marshall sign rule and the phase string effect.

[27] Verges, J. A., Louis, E., Lomdahl, P. S., Guinea, F. & Bishop, A. R. Holes and magnetic textures in the two-dimensional Hubbard model. *Phys. Rev. B* **43,** 6099-6108 (1991).

[28] Berciu, M. & John, S. Numerical study of multisoliton configurations in a doped antiferromagnetic Mott insulator. *Phys. Rev. B* **59,** 15143-15159 (1999).

[29] Morinari, T. Half-skyrmion picture for high-temperature superconductivity and its simulation in cold atoms. *J. Phys. B*: *At. Mol. Opt. Phys.* **39**, S37-S45 (2006).

[30] Morinari, T. Half-skyrmion picture of a single-hole-doped CuO_2 plane. *Phys. Rev. B* **72,** 104502 (2005).

[31] Kou, S.-P. & Weng, Z.-Y. Topological gauge structure and phase diagram for weakly doped antiferromagnets. *Phys. Rev. Lett.* **90,** 157003 (2003).

[32] Kou, S.-P. & Weng, Z.-Y. Holes as dipoles in a doped antiferromagnet and stripe instabilities. *Phys. Rev. B* **67,** 115103 (2003).

[33] Kou, S.-P. & Weng, Z.-Y. Self-localization of holes in a lightly doped Mott insulator. *Eur. Phys. J. B* **47**, 37–46 (2005)

[34] Shraiman, B. & Siggia, E. Mobile vacancies in a quantum Heisenberg antiferromagnet. *Phys. Rev. Lett.* **61,** 467-470 (1988), *ibid.* Spiral phase of a doped quantum antiferromagnet. *Phys. Rev. Lett.* **62,** 1564-1567 (1989).

[35] Timm, C. & Bennemnn, K. H. Doping dependence of the Néel temperature in Mott-Hubbard antiferromagnets: effect of vortices. *Phys. Rev. Lett.* **84,** 4994-4997 (2000).

[36] Glazman, L. I. & Ioselevich, A. S. Theory of the reentrant transition in a lamellar antiferromagnet: doped La_2CuO_4. *Z. Phys. B*: *Condensed Matter* **80,** 133 (1990).

[37] Aharony, A., Birgeneau, R. J., Coniglio, A., Kastner, M. A. & Stanley, H. E. Magnetic phase diagram and magnetic pairing in doped La_2CuO_4. *Phys. Rev. Lett.* **60,** 1330-1333 (1988).

[38] Cherepanov, V., Korenblit, I. Y., Aharony, A. & Entin-Wohlman O. Suppression of antiferromagnetic correlations by quenched dipole–type impurities. *Eur. Phys. J. B*: *Condensed Matter and Complex Systems* **8,** 511-523 (1999).

[39] Beach, K. S. D. & Gooding, R. J. Spin twists, domain walls, and the cluster spin-glass phase of weakly doped cuprates. *Eur. Phys. J. B*: *Condensed Matter and Complex Systems* **16,** 579-591 (2000).

[40] Salem, N. M. & Gooding, R. J. The annealed positions of ferromagnetic bonds doped into a 2D antiferromagnet. *Europhys. Lett.* **35,** 603-608 (1996).

[41] Weng, Z.-Y., Sheng, D.-N. & Ting, C.-S., Spin-charge separation in the t-J model: magnetic and transport anomalies. *Phys. Rev. B* **52,** 637-664 (1995).

[42] Lee, P. A., Nagaosa, N. & Wen, X.-G. Doping a Mott insulator: physics of high temperature superconductivity. *Rev. Mod. Phys.* **78,** 17-87 (2006) and reference therein.

[43] Rey, A. M, Blakie, P. B., Pupillo, G., Williams, C. J. & Clark C. W. Bragg spectroscopy of ultracold atoms loaded in an optical lattice. *Phys. Rev. A* **72,** 023407 (2005).

[44] Gerbier, F. et al. Expansion of a quantum gas released from an optical lattice. arXiv: 0808.2212, and references therein.

[45] Bruun, G. M., Andersen, B. M., Demler, E. & Søensen, A. S. Probing spatial spin correlations of ultracold gases by quantum noise spectroscopy. arXiv: 0809.0312.

[46] Guarrera, V. et al. Noise correlation spectroscopy of the broken order of a Mott insulating phase. arXiv: 0803.2015.

[47] Köhl, M., Moritz, H., Stöferle, T. Günter, K. & Esslinger, T. Fermionic Atoms in a Three Dimensional Optical Lattice: Observing Fermi Surfaces, Dynamics, and Interactions. *Phys. Rev. Lett.* **94,** 080403 (2005).

[48] Lindner, N., Auerbach, A. & Arovas, D. P., Emergence of spin-half fermion vortices and the vortex metal. arXiv: cond-mat/0701571.

[49] Barthel, T., Kaszetelan, C., McCulloch I. P. & Schollwöck, U. Magnetism, coherent many-particle dynamics, and relaxation with ultracold bosons in optical superlattices. arXiv: 0809.5141.

[50] Akpojotor, G. E. & Li, W., Testing of spin ordering Hamiltonian with ultracold atoms in optical lattices. arXiv: 0810.4363.